Engineering Structures 144 (2017) 19–25

Contents lists available at ScienceDirect

Engineering Structures

journal homepage: www.elsevier.com/locate/engstruct

A theoretical model for a piezoelectric energy harvester with a tapered shape

X.D. Xie [a], A. Carpinteri [b], Q. Wang [a,*]

[a] Department of Architecture and Civil Engineering, City University of Hong Kong, Kowloon, Hong Kong Special Administrative Region
[b] Department of Structural, Geotechnical and Building Engineering, Politecnico di Torino, Corso Duca degli Abruzzi, Italy

ARTICLE INFO

Article history:
Received 22 February 2017
Revised 6 April 2017
Accepted 6 April 2017
Available online 4 May 2017

Keywords:
Piezoelectric coupled energy harvester
Tapered cantilever
Finite differential method

ABSTRACT

A piezoelectric energy harvester made of a tapered cantilever surface bonded with piezoelectric patches is developed to harness energy from ambient vibrations. Compared with the available cantilever harvester of a uniform shape in the length direction, this harvester has a higher energy harvesting efficiency since a maximum collected power at each piezoelectric patch on the cantilever can be achieved. The current available models for cantilever harvesters are not applicable for the new developed tapered harvester due to the difficulties in dealing with the tapered shape. A corresponding finite differential model is hence developed to model the tapered harvester for estimating its efficiency by examining a governing differential equation with variable coefficients. The influences of some practical considerations, such as the geometry of the tapered cantilever and the width of piezoelectric patches on the root mean square of the generated electric power, are discussed. The results from the developed model show that an electric power up to 70 times higher than the available uniform cantilever harvesters can be achieved by the tapered harvester. This research provides an effective model for evaluating the high efficiency of the piezoelectric coupled tapered cantilevers in energy harvesting.

1. Introduction

Piezoelectric energy harvesting devices converting ambient energy into electrical energy have attracted much interest in both the academia and industry. Their applications include wearable electronics, where energy harvesting devices can power or recharge cellphones, mobile computers, radio communication equipment, high power output devices (or arrays of such devices) deployed at remote locations to serve as reliable power stations for large systems. The most common type of piezoelectric devices is the piezoelectric/metal sandwich beam mounted as a cantilever due to three major considerations. First, large mechanical strains can be produced directly owing to the piezoelectric effect of the materials during vibrations. Second, the construction of piezoelectric cantilevers is simpler compared to other harvesters. Third, the resonance frequency of the fundamental flexural modes of a cantilever is much lower than the other vibration modes of the piezoelectric element. So far, studies on piezoelectric energy harvesting technologies reported to date have involves a unimorph or bimorph cantilever design [1–5].

The exact expressions for the voltage, current, power, and tip deflection of a Timoshenko piezoelectric cantilever were derived [6]. Subsequently, several case studies were presented to examine the frequency response of vibration-based energy harvesters using this model. An analytical approach based on the Euler–Bernoulli beam theory and Timoshenko beam equations for the voltage and power generation was provided and compared with the electrical equivalent circuit and energy method [7]. The technique to adjust the performance of a piezoelectric bimorph vibrating in the flexural mode through axial preloads was studied to effectively scavenge energy from ambient mechanical vibrations/noise with varying-frequency spectra [8]. Based on a design of a bimorph cantilever located at an arbitrary position on a simply supported slender bridge, a piezoelectric power generation from moving loads was formulated [9]. An optimal design of a piezoelectric coupled cantilever structure attached by a proof mass subjected to seismic motion was introduced to achieve a higher efficient energy harvesting from high-rise buildings [10]. Two types of sea wave piezoelectric cantilever energy harvesters with proof masses were introduced and optimized to harvest electric energy from longitudinal or transverse wave motions of water particles [11,12]. Their results show that the harvesters can generate a power up to 55 W and 30 W for a practical longitudinal and transverse wave motions, respectively. A novel piezoelectric energy harvester

* Corresponding author.
E-mail address: quanwang@cityu.edu.hk (Q. Wang).

http://dx.doi.org/10.1016/j.engstruct.2017.04.050
0141-0296/

device driven by a cantilever system to harvest energy from high-rise buildings was demonstrated [13,14]. This harvester can provide an efficient and practical energy harvesting in the process of dissipating the vibration energy of high-rise buildings. Dhakar et al. [15] proposed a 21-mm-long polymer extension beam with a proof mass of 0.72 g at its free end. The other end of the beam is clamped firmly to the free end of a 32-mm-long PZT-5A bimorph cantilever. Results showed that this design can tune the natural frequencies of the combinational cantilever notably. Azizi et al. [16] investigated the mechanical behavior of a bimorph piezoelectric micro cantilever exposed to harmonic base excitation, and the effect of load resistance and the effective piezoelectric stress constant on the equivalent damping ratio of output circuits including parallel and series connections. The effect of the impact of water droplets releasing from different various heights on the piezoelectric energy harvesting was studied [17] and the results show that a power output for one unit at around 2.5 μW. An auxiliary cantilever with a piezoelectric patch glued at its fixed end subjected to a resonance was conducted to improve power output [18]. Another innovative S-shaped meandering cantilever was designed to achieve a low resonance frequency below 30 Hz by reducing the stiffness of the beam [19]. A two-stage design was proposed in which a spring-mass system was designed to respond at the input frequency of the host structure, and then excite an array of piezoelectric cantilevers to harvest the mechanical energy [20]. A theoretical study of a similar two-stage piezoelectric energy harvester for human walking was conducted. In the study, ferromagnetic structures were used to tune the natural frequency of a piezoelectric cantilever with a magnetic proof mass [21]. Liu etc. [22] presented a power generator array based on thick-film piezoelectric cantilevers with different resonance frequencies to improve frequency flexibility and power output. The cantilever array can be tuned to the frequency and expanded the excited frequency bandwidth in ambient low frequency vibration. Xu et al. [23] presented a low frequency piezoelectric energy harvester "CANDLE" consisting of cantilever beam and cymbal transducers based on piezoelectric single crystal. The design uses a cantilever as the driving mechanism for two cymbal transducers to generate electrical energy.

Three major principles used in the available piezoelectric cantilever harvesters mentioned above to improve their power output are: (1) decreasing the natural frequency of the cantilever device by using a proof mass attached to its free end or a combination beam; (2) enhancing the excitation frequency to the vicinity of the natural frequency of the cantilever by a tuned resonance device; and (3) broadening the band response with respect to the excitation from the host structures. In the aforementioned energy harvester designs, the common intention is to make the piezoelectric coupled cantilever working at the resonance to achieve a maximum power output. However, many ambient vibration sources possess a spectrum of random frequencies. In these situations, tuning a piezoelectric energy harvester to a specific resonance frequency may not be an effective approach to improve efficiency because even a small amount of fluctuation in the input frequency will result in a large drop in the power output. Meanwhile, the tuned frequency device and proof mass may also increase the space and weight of the energy harvester device, and hence decrease the efficiency of the harvesters. And more importantly, the above-mentioned harvester devices only fully use the maximum strain at the fixed end which leaves the piezoelectric material under-utilized, resulting in sub-optimal efficiency [24].

The electrical energy from a piezoelectric material is proportional to the induced mechanical strain. Hence it is desirable to maximize the strain at each point in a beam to fully utilize the potential energy in piezoelectric materials. Under an optimal condition, the strain distribution in the beam would be completely uniform within the strain limit. The consideration suggests a triangular or trapezoidal shape cantilever which has a linearly increased wider cross-section, while reducing the size and weight of a piezoelectric cantilever. Baker et al. [25] introduced a piezoelectric harvester prototype made of a trapezoidal geometry cantilever by finite element method to examine the effect of geometry of the cantilevered piezoelectric beam on the power density. The results showed that the output power is 50% higher than that of a comparable rectangular cantilever with an even strain distribution throughout the beam. Glynne-Jones et al. [26] built a prototype of a thick-film PZT coupling trapezoidal cantilever, and then studied the effect of the load resistance and beam amplitude on the power output of the harvester. Mateu and Moll [27] provided a comprehensive study on a triangular piezoelectric bending beam structure for energy harvesting using shoe inserts. The results showed that by using a triangular cantilever, the strain along axial direction is made to be a constant and the harvested energy increases with an increase in the thickness of the triangular cantilever. Roundy [28] provided a relationship between the relative bending energies and strain profiles for alternative cantilever geometries, and found that a trapezoidal geometry can supply more than twice of the energy (per unit volume PZT) than the rectangular geometry. Reducing the coupled governing differential equations with variable coefficients to a pair of uncoupled second-order differential equations, Yuan et al. [29] simplified the governing equations for the free vibration of circular Timoshenko beams with both geometrical nonuniformity and material inhomogeneity along the beam axis and derived a series of exact analytical solutions from the reduced equations for the first time.

These researches aforementioned on cantilever energy harvester with varying cross-sectional area use either simulation or model testing, and focus on the cantilever tapering in the width because there is no analytical solution to the dynamic governing equations of the piezoelectric coupled cantilever tapering in both width and thickness directions. In fact, a taper in thickness of a cantilever has a greater contribution on the surface strain of the cantilever than that from the taper in width.

It is hence expected to develop a mathematical model for a tapered cantilever energy harvester in both width and thickness directions to harvest energy from ambient vibration. With this novel model, the effect of the taper in width and/or thickness of the cantilever, the width of the pzt patches, the width and the thickness at the fixed end of the cantilever on the energy harvesting efficiency of the tapered harvester can be studied comprehensively. The research findings are significant and helpful in designing the most efficient and economic piezoelectric coupled tapered cantilever energy harvesters which can maximize the surface strain at each point in the beam to harvest the strain energy at a fullest extent.

2. Introduction of the analytical model

The introduction of a piezoelectric coupled cantilever harvester with a rectangular cross section tapered in both thickness and width is depicted in Fig. 1(a and b). The cantilever is subjected to a sinusoidal force $F = Y\sin\omega' t$ at its free end. Fig. 1a schematically illustrates the normal section view of the harvester with a length of l. it is tapered in the thickness direction from h_0 at the fixed end to h_1 at the free end, and attached by pzt4 patches with the same thickness of t_p one by one on the upper and lower surfaces of the cantilever. Fig. 1b is the top view of the harvester tapered in the width direction from b_0 at the fixed end to b_1 at the free end. The attached individual pzt4 patches fully on the surfaces of the cantilever are with a varying length $l_p(x)$. Based on the model

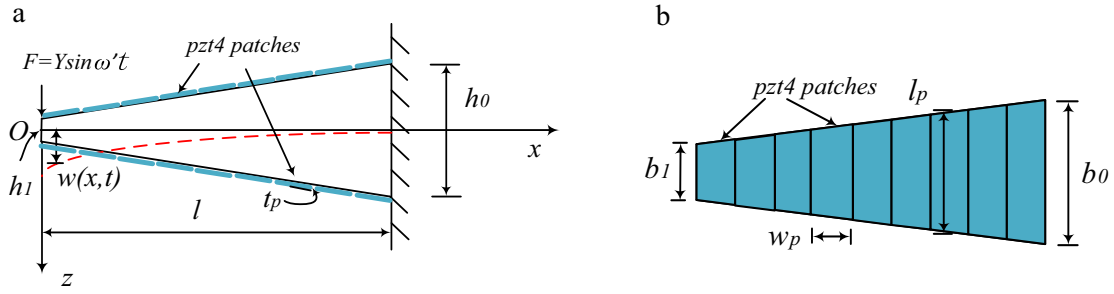

Fig. 1. Set-up of a piezoelectric energy harvester. (a) Normal section view, (b) Top view.

in Fig. 1, a mathematical model for the piezoelectric tapered cantilever energy harvester is developed and solved by a finite differential method to evaluate the efficiency of the developed harvester.

3. Development of the theoretical model

The electric power of the piezoelectric coupled cantilever can be studied by setting an excitation of a harmonic sinusoidal wave as a simple representative of the ambient vibration. Therefore, the harmonic motion on the cantilever is set to be, $f(x,t) = F(t)\delta(x) = \delta(x)\, Y \sin\omega' t$, where Y is the amplitude of the ambient excitation; ω' is the angular frequency of the excitation; $\delta(x)$ is the Kronecker Delta function to represent a point force in beam models. Such a modeling for a point force should also be adopted in another work by the authors [30] although the research findings remain similar.

The motion equation for the forced lateral vibration of the piezoelectric coupled tapered cantilever can be expressed as:

$$\frac{\partial^2}{\partial x^2}\left[EI(x)\frac{\partial^2 w(x,t)}{\partial x^2}\right] + m(x)\frac{\partial^2 w(x,t)}{\partial t^2} = F(t)\delta(x) \quad 0 \leqslant x \leqslant l \tag{1}$$

It is assumed that the piezoelectric patches are bonded on the surfaces of the tapered cantilever. When bending motion takes place on the cantilever subjected to the excitation force, the generated charge Q_g and voltage V_g as well as the electric power of the piezoelectric patches are hence provided as below [31]:

$$Q_g(t) = -e_{31}\sum_{i=1}^{m}\left(\int_{(i-1)w_p}^{iw_p} b(x)(h(x)+2h_p)\frac{d^2w}{dx^2}dx\right), \tag{2}$$

$$V_g(t) = \sum_{i=1}^{m}\frac{Q_g^i(t)}{C_V} = -\frac{e_{31}}{2C'_V}\sum_{i=1}^{m}\int_{(i-1)w_p}^{iw_p}(h(x)+2h_p)\frac{d^2w}{dx^2}dx, \tag{3}$$

$$P_e(t) = \sum_{i=1}^{m}\frac{dQ_g^i(t)}{dt}V_g^i(t), \tag{4}$$

where e_{31} is the piezoelectric constant; $w(x, t)$ is the transverse displacement of the tapered cantilever; C_V is the electrical capacity of the piezoelectric patch; and C'_V is the electric capacity per unit width of the piezoelectric patch ($C'_V = C_V/l_p(x)$), m is the number of piezoelectric patches bonded on the upper and lower surfaces of the tapered cantilever.

To obtain the time varying displacement field, $w(x, t)$, in Eq. (1) by the classical elastic beam model, the cantilever is simply separated into $m/2$ sections, as shown in Fig. 1, by considering each piezoelectric bonded area connected each other. Based on the Euler-Bernoulli beam theory, the vibration governing equation for the tapered cantilever can be expressed as:

$$EI_0\frac{\partial^2}{\partial x^2}\left[u\nu^3\frac{\partial^2 w(x,t)}{\partial x^2}\right] + m_0 u\nu\frac{\partial^2 w(x,t)}{\partial t^2} = 0 \tag{5}$$

where, $m_0 = \rho b_0 h_0$, $I_0 = \frac{b_0 h_0^3}{12}$, $u = [\alpha + (1-\alpha)\frac{x}{l}]$, $\nu = [\beta + (1-\beta)\frac{x}{l}]$, $\alpha = b_1/b_0$, $\beta = h_1/h_0$.

In order to obtain the natural frequencies and corresponding vibration shapes of the tapered cantilever, we use the modal method:

$$w(x,t) = \sum_{n=1}^{\infty} W_n(x)q_n(t), \tag{6}$$

Substitution of Eq. (6) into Eq. (5) leads to the following expression:

$$\frac{d^4W}{dx^4} + a_1(x)\frac{d^3W}{dx^3} + a_2(x)\frac{d^2W}{dx^2} + a_3(x)W = 0, \tag{7}$$

in which, $a_1(x) = 2\{\frac{1-\alpha}{ul} + 3\frac{1-\beta}{\nu l}\}$, $a_2(x) = 6\frac{1-\beta}{l}\{\frac{1-\alpha}{u\nu l} + \frac{1-\beta}{\nu^2 L}\}$, $a_3(x) = -\frac{m_0\omega^2}{\nu^2 EI_0}$.

Since there is no analytical solution for the Eq. (7), here the finite differential method is used to obtain the natural frequencies and corresponding vibration shapes of the tapered cantilever.

For the tapered cantilever, the boundary conditions are as below:

$$\left.\begin{aligned} &W''(0) = 0, (EIW'')'|_0 = EI'(0)W''(0) + EI(0)W(0)''' = 0 \\ &W'(l) = 0, W(l) = 0 \end{aligned}\right\} \tag{8}$$

By expressing the first three order derivatives of the boundary points by Taylor Series, then the boundary conditions can be expressed as:

$$\frac{2}{h^2}W_1 - \frac{5}{h^2}W_2 + \frac{4}{h^2}W_3 - \frac{1}{h^2}W_4 = 0, \tag{9}$$

$$-\frac{1}{h^3}W_1 + \frac{3}{h^3}W_2 - \frac{3}{h^3}W_3 + \frac{1}{h^3}W_4 = 0, \tag{10}$$

$$-\frac{1}{3h}W_{n-3} + \frac{3}{2h}W_{n-2} - \frac{3}{h}W_{n-1} + \frac{11}{6h}W_n = 0 \tag{11}$$

$$W_n = 0 \tag{12}$$

in which, $h = \frac{l}{n-1}$, n is the number of discrete points on the tapered cantilever including the free end and fixed end points, $W_{1\sim4}$ and $W_{n\text{-}3\sim n}$ are the displacements of the vibration shape at corresponding discrete points on the tapered cantilever.

By expressing the first four order derivatives of the internal points by central differential formula, the finite differential equations of the internal points can be expressed as:

$$Z_{1i}W_{i-2}+Z_{2i}W_{i-1}+Z_{3i}W_i+Z_{4i}W_{i+1}+Z_{5i}W_{i+2}=0 \quad (3\leqslant i\leqslant n-2) \tag{13}$$

in which, $Z_{1i}=\frac{1}{h^4}-\frac{a_1(x_i)}{2h^3}$, $Z_{2i}=-\frac{4}{h^4}+\frac{a_1(x_i)}{h^3}+\frac{a_2(x_i)}{h^2}$, $Z_{3i}=\frac{6}{h^4}-\frac{2a_2(x_i)}{h^2}+a_3(x_i)$, $Z_{4i}=-\frac{4}{h^4}-\frac{a_1(x_i)}{h^3}+\frac{a_2(x_i)}{h^2}$, $Z_{5i}=\frac{1}{h^4}+\frac{a_1(x_i)}{2h^3}$, $x_i=(i-1)h$. In order to obtain the value of the vibration shape at each discrete point, let $W(0)=W_1=1$, then the formula of $W_{2\sim n}$ can be derived based on Eqs. (9)–(12) and (13).

$$W_2=U_2W_4+V_2, \tag{14}$$

$$W_3=U_3W_4+V_3, \tag{15}$$

$$W_{i+1}=U_{i+1}W_{i+2}+V_{i+1} \quad 3\leqslant i\leqslant n-2, \tag{16}$$

$$W_n=V_n, \tag{17}$$

The expressions of U_i and V_i can be seen in Appendix.Let $V_n=0$, each natural frequency can be obtained by iteration method, and then the corresponding vibration shape can be achieved through back substituting natural frequency into Eqs. (16) and (17). So the generalized coordinates can also be obtained below:

$$q_n=\frac{C}{Bm_0(\omega_n^2-\omega'^2)}\sin\omega' t, \tag{18}$$

in which, $B=\int_0^l W_n^2(x)dx$, $C=W_n(0)Y/\alpha\beta$.

Substitution of Eq. (18) into Eq. (6) and Eq. (6) into Eqs. (2)–(4) lead to the expressions of the electric power $P_e(t)$. Further the RMS (root mean square) of the generated power from *0* to *t/4* from the piezoelectric patches can be obtained as:

$$P_e^{rms}=2\sqrt{\frac{4}{t}\int_0^{t/4}[P_e(\tau)]^2d\tau}, \tag{19}$$

where $P_e(\tau)$ is the generated power of the piezoelectric coupled tapered cantilever harvester at time τ (0 < τ < t/4).

To estimate the RMS of the generated power, the period, *t/4*, can be separated into j time steps with a sufficiently short time interval Δt. As a result, the expression in Eq. (19) can be rewritten in a discrete form below:

$$P_e^{rms}=4\sqrt{\frac{\Delta t}{t}\sum_{i=1}^{j}[P_e(t_i)]^2} \tag{20}$$

4. Results and discussions

Based on the finite differential model developed in Section 3, the generated charge, voltage and electric power from the piezoelectric patches can be obtained. In this section, we conduct simulations to study the effects of the taper ratios in both thickness and width of the cantilever, the width of piezoelectric patches, the width and thickness at the fixed end of the cantilever on the harvester power. The dimensions and materials properties of the piezoelectric coupled cantilever in the simulations are provided in Table 1, unless otherwise noted. The amplitude of the harmonic

Table 1
Material properties and dimensions of a piezoelectric coupled tapered cantilever energy harvester.

Tapered cantilever							PZT4 patches			
l(m)	*b_0(m)*	*h_0(m)*	*α*	*β*	*E(N/m^2)*	*ρ (kg/m^3)*	*w_p(cm)*	*t_p(mm)*	*ρ(kg/m^3)*	*e_{31} (C/m^2)*
0.6	*0.04*	*0.003*	*0.2–1.0*	*0.2–1.0*	*2.1e11*	*7800*	*1–6*	*0.3*	*7500*	*−2.8*
C_v (nF)	0.75 for the piezoelectric patch with the geometry of *0.01, 0.06, 0.0003* m									

Table 2
Natural frequencies of cantilever beam with different parameters β.

N = 601	α = 1,β = 1 ω_1	α = 1,β = 1 ω_2	α = 1,β = 1 ω_3	α = 1,β = 0 ω_1
Calculating solution	44.11	276.41	773.97	66.35
Analytical solution[31]	43.89	275.04	770.12	66.34
Tolerance	0.501%	0.498%	0.499%	0.015%

Note: E = 2.1e11, b0 = 0.04m, h0 = 0.003m, $\alpha = b_1/b_0$, $\beta = h_1/h_0$.

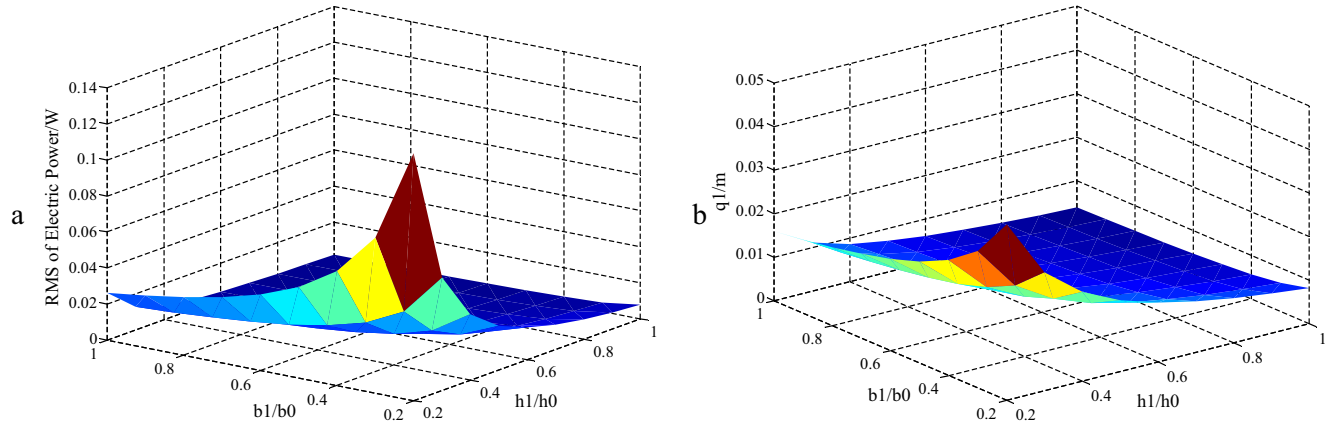

Fig. 2. RMS of the electric power and amplitude of q_1 versus the taper ratios of the cantilever harvester. (a) RMS versus b_1/b_0 and h_1/h_0, (b) Amplitude of q_1 versus b_1/b_0 and h_1/h_0.

excitation, Y, is set to be 1 N to assure a safe operation of the harvester without losing any generality. The piezoelectric patches and the host cantilever beam are made of PZT4 (lead zirconate titanate) and steel, respectively.

Firstly, to verify the effectiveness of the developed finite difference method, we set $\alpha = 1$, $\beta = 1$ and $\alpha = 1$, $\beta = 0$ to study a pure uniform cantilever and a pure tapered cantilever, respectively. The corresponding natural frequencies of the cantilever are calculated by finite differential method taking the discrete point number of $n = 601$, and compared to the analytical solutions. The results (see in Table 2) show that the finite differential method has a good precision.

Fig.2 shows the effect of the taper ratios in width and thickness of the cantilever on the RMS of electric power and the amplitude of first generalized coordinate of the cantilever harvester. The parameters in this simulation are set to be: $n = 601$, $b0 = 0.04$ m, $h0 = 0.003$ m, $l = 0.6$ m, $w_p = 0.012$ m, $Y = 1$ N, and $\omega' = 10$ rad/s. Fig. 2a displays that the RMS nonlinearly decreases from 0.1376 W to 0.0263 W, 0.1376 W to 0.0077 W, and 0.1376 W to 0.002 W when the width ratio of b_1/b_0 and the thickness ratio of h_1/h_0 change from (0.2, 0.2) to (1.0, 0.2), (0.2, 0.2) to (0.2, 1.0), and (0.2, 0.2) to (1.0, 1.0), respectively. It also shows that the RMS, at $b_1/b_0 = h_1/h_0 = 0.2$, is 70 times of the RMS at $b_1/b_0 = h_1/h_0 = 1.0$, and 17.9 times of that at $b_1/b_0 = 0.2$ and $h_1/h_0 = 1.0$, and 5.2 times of that at $b_1/b_0 = 1.0$ and $h_1/h_0 = 0.2$, respectively. Similarly, the amplitude of the first generalized coordinate decreases as shown in Fig. 2b from 0.0405 m to 0.0159 m, 0.0405 m to 0.0082 m, and 0.0405 m to 0.0038 m when b_1/b_0 and h_1/h_0 change from (0.2, 0.2) to (1.0, 0.2), (0.2, 0.2) to (0.2, 1.0), and (0.2, 0.2) to (1.0, 1.0), respectively. The findings on the decrease in RMS with increases in the ratios are mainly caused by the similar change of the first generalized coordinate q_1. A nonlinear increase in q_1 can lead to a nonlinear increase in the electric power as shown in Eqs. (6), (2)–(4). The results indicate that the taper ratio in thickness has a more obvious effect on the RMS than the taper ratio in width of the cantilever. More importantly, the results show that the tapered cantilever harvester has a much higher energy harvesting efficiency and is more economic than the counterpart uniform cantilever.

Fig.3 illustrates the variation of RMS of the generated power and the amplitude of the sum of voltage on the piezoelectric patches versus the width of pzt4 patch with the following parameters: $n = 601$, $b0 = 0.04$ m, $h0 = 0.003$ m, $l = 0.6$ m, $h_1/h_0 = 1.0$, and $b_1/b_0 = 0.2$. It can be seen from the Fig. 3a that the RMS nonlinearly decreases from 0.1376 W to 0.1354 W when the pzt4 width changes from 0.01 m to 0.06 m. This phenomenon is mainly because the increase in the width of pzt4 patch would cause an increase in C_v, which in turn causes a decrease in the voltage and electric power as shown in Eqs. (3) and (4). As we can see from Fig. 3b, the amplitude of the sum of voltage on the piezoelectric patches similarly decreases from 1074 V to 1050 V in this range. This finding indicates that a larger energy harvesting requires a

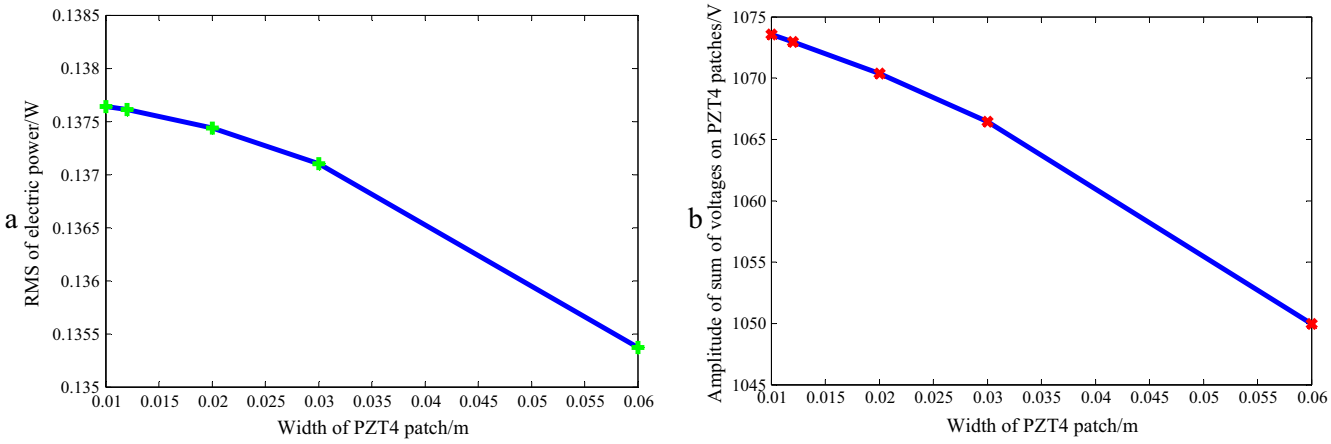

Fig. 3. RMS of the electric power and the amplitude of sum of voltage of pzt4 patches versus the width of pzt4 patch. (a) RMS versus the width of pzt4 patch, (b) Amplitude of sum of voltage of pzt4 patches versus the width of pzt4 patch.

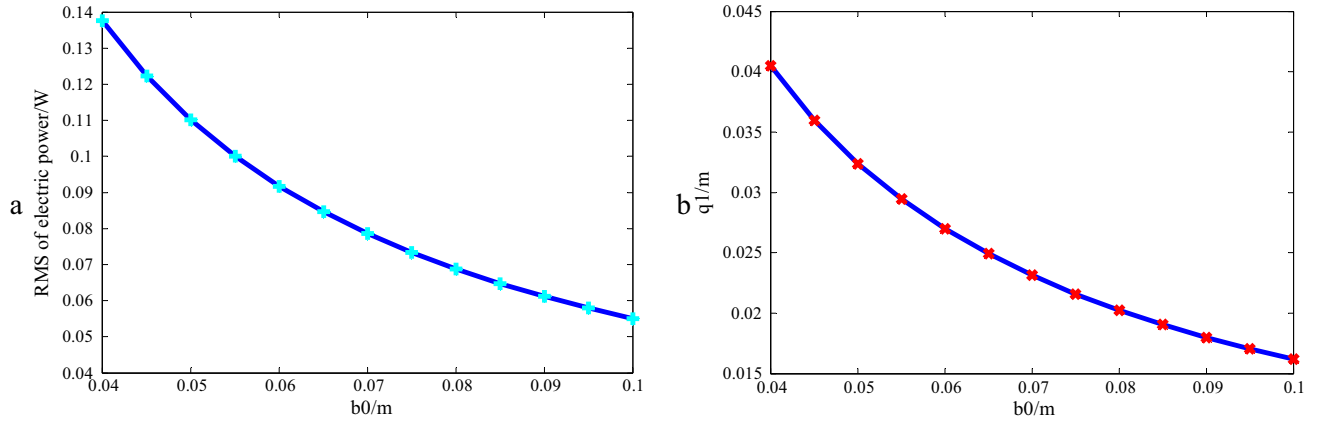

Fig. 4. RMS of the electric power and amplitude of sum of current of pzt4 patches versus the fixed end width of harvester. (a) RMS versus fixed end width of harvester, (b) Amplitude of q_1 versus fixed end width of harvester.

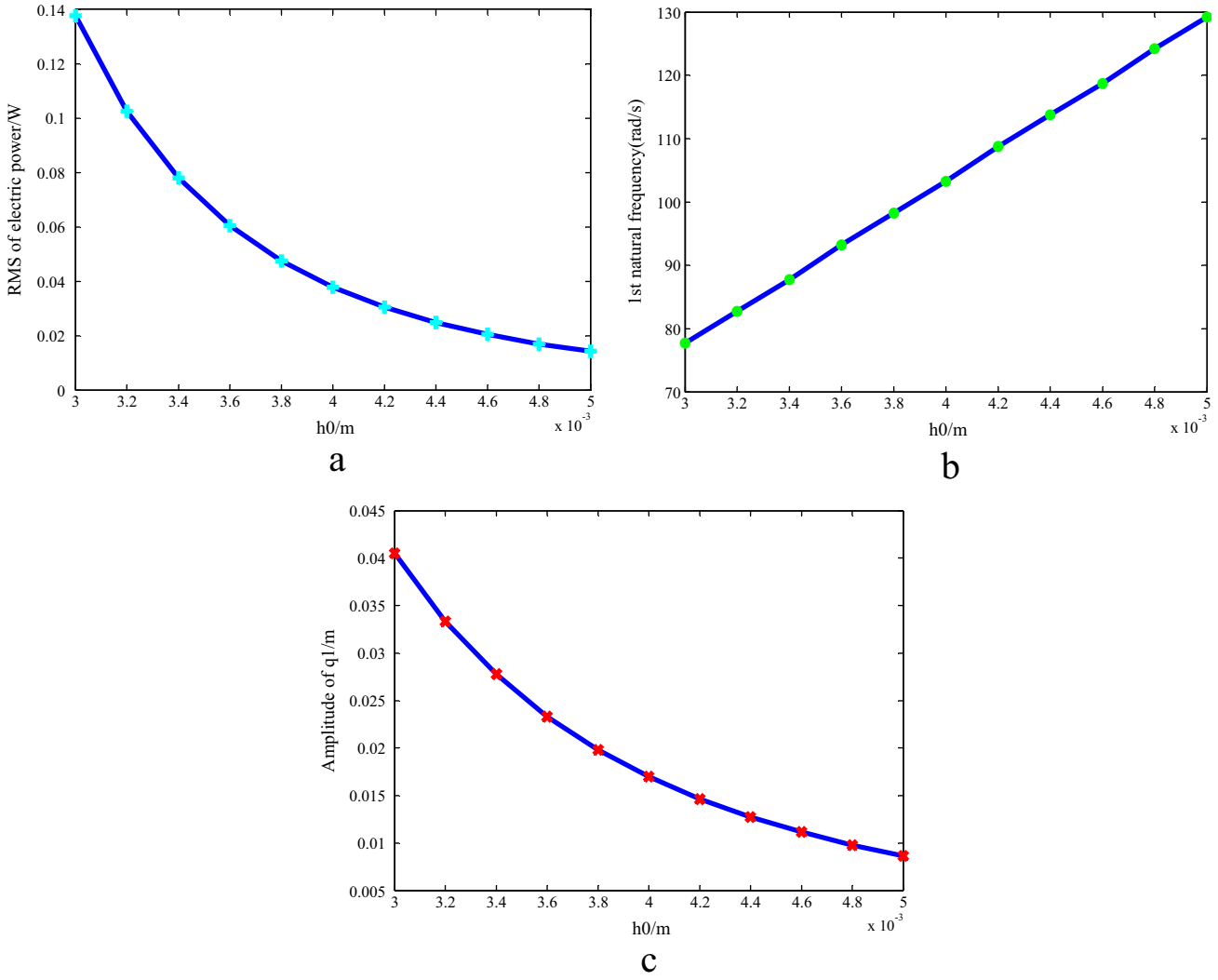

Fig. 5. RMS of the electric power, amplitudes of surface curvature difference of the harvester, and q_1 versus the fixed end thickness of the harvester. (a) RMS versus fixed end thickness of the harvester, (b) 1st natural frequency versus fixed end thickness of the harvester, (c) Amplitude of q_1 versus fixed end thickness of the harvester.

series of piezoelectric patches with a smaller width based on the theoretical model.

Fig. 4 demonstrates the effect of the width at the fixed end of the cantilever on the RMS and the amplitude of the first generalized coordinate with the parameters: n = 601, h0 = 0.003 m, l = 0.6 m, and $h_1/h_0 = b_1/b_0 = 0.2$. Fig. 4a shows a nonlinear decrease in RMS from 0.1376 W to 0.055 W under the condition of the width at the fixed end of the cantilever changing from 0.04 m to 0.1 m. The findings on the decrease in RMS with an increase in the width at the fixed end of the cantilever are owing to the fact that an increase in b_0 would lead to an increase in the mass, $m_0 = \rho b_0 h_0$, and hence the decreases in the amplitude of generalized coordinates, q_1, the voltage on PZT4 patches, V_g, and the electric power, P_e, which can be seen from Eqs. (18), (3) and (4). For example, the amplitude of q_1 nonlinearly decreases from 0.036 m to 0.016 m in the same section shown in the Fig. 4b. This result suggests that a smaller b_0 for the tapered cantilever harvester will lead to more electric power harvesting from the same ambient excitation.

Fig. 5 displays the effect of the thickness at the fixed end of the cantilever on the RMS, the first generalized coordinate and the first natural frequency of the cantilever. The dimensions of the energy harvester in this simulation are set to be, n = 601, b0 = 0.04 m, l = 0.6 m, and $h_1/h_0 = b_1/b_0 = 0.2$. From Fig. 5a it can be found that the RMS nonlinearly decreases from 0.1376 W to 0.0142 W with an increase in the thickness at the fixed end of the cantilever from 3 mm to 5 mm. This phenomenon is caused by the similarly variational tendency in the amplitude of the first generalized coordinate which is relevant to two factors. The main factor is the linearly increase in the first natural frequency of the tapered harvester from 77.75 rad/s to 129.25 rad/s in the same thickness section which can be seen from Fig. 5b; the second factor is the linearly increase in the mass of $m_0 = \rho b_0 h_0$. Two reasons above lead to a nonlinearly decrease in the amplitude of the first generalized coordinate from 0.0405 m to 0.0087 m shown as Fig. 5c. These phenomena in Fig. 5 can also be explained explicitly by Eqs. (18) and (2)–(4). The results reveal that a thicker cantilever harvester with the same taper ratio in thickness would lead to a decrease of RMS significantly.

5. Conclusion

A piezoelectric energy harvester made of a tapered cantilever surface bonded with piezoelectric patches is developed to harness energy from ambient vibrations. The current available models for

cantilever harvesters are not applicable for the new developed tapered harvester due to the difficulties in dealing with the tapered shape. A corresponding finite differential model is hence developed to model the tapered harvester for estimating its efficiency by examining a governing differential equation with variable coefficients. Numerical simulation results from the model show that the RMS decreases with an increase in the taper ratio of thickness and/or width of the cantilever and the width of the PZT4 patch, and an increase in the thickness and/or width at the fixed end of the cantilever. For an energy harvester structure with geometry and material parameters of $b0 = 0.04$ m, $h0 = 0.003$ m, $l = 0.6$ m, $b_1/b_0 = h_1/h_0 = 0.2$, $w_p = 0.012$ m, $tp = 0.3$ mm, $Y = 1$ m and $\omega' = 10$ rad/s, the RMS can reach up to 0.1376 W which is 70 times of the uniform counterpart. The research develops a novel technique to improve the efficiency of energy harvesters to the fullest extent.

Appendix A.

$$U_2 = \frac{1}{\Delta_2 h^5}, V_2 = \frac{2}{\Delta_2 h^5}, U_3 = \frac{2}{\Delta_2 h^5}, V_3 = \frac{1}{\Delta_2 h^5}, \Delta_2 = \Delta_3 = \frac{3}{h^5}.$$

$$U_4 = \frac{-Z_{53}}{\Delta_4},\ V_4 = \frac{-1}{\Delta_4}[Z_{13}W_1 + Z_{23}V_2 + Z_{33}V_3],\ \Delta_4 = Z_{23}U_2 + Z_{33}U_3 + Z_{43}.$$

$$U_5 = \frac{-Z_{54}}{\Delta_5}, V_5 = \frac{-1}{\Delta_5}[Z_{14}V_2 + Z_{24}V_3 + (Z_{14}U_2 + Z_{24}U_3 + Z_{34})V_4], \Delta_5 = (Z_{14}U_2 + Z_{24}U_3 + Z_{34})U_4 + Z_{44}.$$

$$U_{i+1} = \frac{-Z_{5i}}{\Delta_{i+1}}, V_{i+1} = \frac{-1}{\Delta_{i+1}}\{Z_{1i}V_{i-2} + (Z_{1i}U_{i-2} + Z_{2i})V_{i-1} + [(Z_{1i}U_{i-2} + Z_{2i})U_{i-1} + Z_{3i}]V_i\},$$

$$\Delta_{i+1} = [U_{i-1}(Z_{2i} + Z_{1i}U_{i-2}) + Z_{3i}]U_i + Z_{4i}.$$

$$V_n = \frac{-1}{\Delta_n}\{Z_{1,n-1}V_{n-3} + (Z_{1,n-1}U_{n-3} + Z_{2,n-1})V_{n-2} + [(Z_{1,n-1}U_{n-3} + Z_{2,n-1})U_{n-2} + Z_{3,n-1}]V_{n-1}\},$$

$$\Delta_n = [U_{n-2}(Z_{2,n-1} + Z_{1,n-1}U_{n-3}) + Z_{3,n-1}]U_{n-1} + Z_{4,n-1}.$$

References

[1] Schoeftner J, Buchberger G. A contribution on the optimal design of a vibrating cantilever in a power harvesting application – optimization of piezoelectric layer distributions in combination with advanced harvesting circuits. Eng Struct 2013;53:92–101.
[2] Shi Z, Li J, Yao R. Solution modification of a piezoelectric bimorph cantilever under loads. Int J Eng Sci 2015;26(15):2028–41.
[3] Gao X, Shih WH, Shih WY. Vibration energy harvesting using piezoelectric unimorph cantilevers with unequal piezoelectric and nonpiezoelectric lengths. Appl Phys Lett 2010;97:233503.
[4] Zhang K, Wang D, Zhou Q. Study on the electromechanical coupling performance of bimorph piezoelectric cantilever. Appl Mech Mater 2013;302:447–51.
[5] Song G, Sethi V, Li H-N. Vibration control of civil structures using piezoceramic smart materials: a review. Eng Struct 2006;28:1513–24.
[6] Dietl JM, Wickenheiser AM, Garcia E. A Timoshenko beam model for cantilevered piezoelectric energy harvesters. Smart Mater Struct 2010;19:055018.
[7] Ajitsaria J, Choe SY, Shen D, Kim DJ. Modeling and analysis of a bimorph piezoelectric cantilever beam for voltage generation. Smart Mater Struct 2007;16:447–54.
[8] Hu Y, Xue H, Hu H. A piezoelectric power harvester with adjustable frequency through axial preloads. Smart Mater Struct 2007;16:1961–6.
[9] Erturk A. Piezoelectric energy harvesting for civil infrastructure system applications: moving loads and surface strain fluctuations. J Intell Mater Syst Struct 2011;22:1959–73.
[10] Xie XD, Wu N, Yuen KV, Wang Q. Energy harvesting from high-rise buildings by a piezoelectric coupled cantilever with a proof mass. Int J Eng Sci 2013;72(11):98–106.
[11] Xie XD, Wang Q, Wu N. Potential of a piezoelectric energy harvester from sea waves. J Sound Vib 2014;333(5):1421–9.
[12] Xie XD, Wang Q, Wu N. Energy harvesting from transverse ocean waves by a piezoelectric plate. Int J Eng Sci 2014;81(8):41–8.
[13] Xie XD, Wang Q, Wang SJ. Energy harvesting from high-rise buildings by a piezoelectric harvester device. Energy 2015;93:1345–52.
[14] Xie XD, Wang Q. Design of a piezoelectric harvester fixed under the roof of a high-rise building. Eng Struct 2016;117:1–9.
[15] Dhakar HC, Liu FE, Tay H, Lee C. A new energy harvester design for high power output at low frequencies. Sens Actuators A 2013;199:344–52.
[16] Azizi S, Ghodsi A, Jafari H, Ghazavi MR. A conceptual study on the dynamics of a piezoelectric MEMS (Micro Electro Mechanical System) energy harvester. Energy 2016;96:495–506.
[17] Ilyas MA, Swingler J. Piezoelectric energy harvesting from raindrop impacts. Energy 2015;90:796–806.
[18] Cornwell PJ, Goethal J, Kowko J, Damianakis M. Enhancing power harvesting using a tuned auxiliary structure. J Intell Mater Syst Struct 2005;16(10):825–34.
[19] Liu C, Lee T, Kobayashi T, Tay C, Quan C. A new S-shaped MEMS PZT cantilever for energy harvesting from low frequency vibrations below 30 Hz. Microsyst Technol 2012;18(4):497–506.
[20] Rastegar J, Pereira C, Nguyen HL. Piezoelectric-based power sources for harvesting energy from platforms with low-frequency vibration. Proc SPIE 2006;6171:617101.
[21] Anderson B, Wickenheiser A. Performance analysis of frequency up-converting energy harvesters for human locomotion. Proc SPIE 2012;8341:834102.
[22] Liu JQ, Fang HB, Xu ZY, Mao XH, Shen XC, Chen D, et al. A MEMS-based piezoelectric power generator array for vibration energy harvesting. Microelectron J 2008;39(5):802–6.
[23] Xu C, Ren B, Di W, Liang Z, Jiao J, Li L, et al. Cantilever driving low frequency piezoelectric energy harvester using single crystal material 0.71Pb(Mg1/3Nb2/3)O3-0.29PbTiO3. Appl Phys Lett 2012;101(3):033502.
[24] Li H, Tian C, Deng D. Energy harvesting from low frequency applications using piezoelectric materials. Appl Phys Rev 2014;1:041301.
[25] Baker J, Roundy S, Wright P. Alternative geometries for increasing power density in vibration energy scavenging for wireless sensor networks. 3rd International Energy Conversion Engineering Conference. San Francisco, California, USA: AIAA; 2005. 2005-5617.
[26] Glynne JP, Beeby SP, White NM. Towards a piezoelectric vibration-powered microgenerator. IEEE Proc 2001;148(2):68–72.
[27] Mateu L, Moll F. Optimum Piezoelectric Bending Beam Structures for Energy Harvesting using Shoe Inserts. J Intell Mater Syst Struct 2005;16(10):835–45.
[28] Roundy S, Leland ES, Baker J, Carleton E, Reilly E, Lai E, et al. Improving power output for vibration-based energy scavengers. IEEE Pervasive Comput 2005;4(1):28–36.
[29] Yuan J, Pao YH, Chen W. Exact solutions for free vibrations of axially inhomogeneous Timoshenko beams with variable cross section. Acta Mech 2016;227:2625–43.
[30] Xie XD, Wang Q. A study on a high efficient cylinder composite piezoelectric energy harvester. Compos Struct 2017;161:237–45.
[31] Lee CK, Moon FC. Modal sensors and actuators. J Appl Mech 1990;57(2):434–41.